Title

NUMERICAL MODELING STUDIES OF THE CERRO PRIETO RESERVOIR

Authors

Lippmann, M.J.
Goyal, K.P.

Publication Date

1980-02-01

LBL-9590
CERRO PRIETO-14

MEXICAN-AMERICAN COOPERATIVE PROGRAM AT THE CERRO PRIETO GEOTHERMAL FIELD

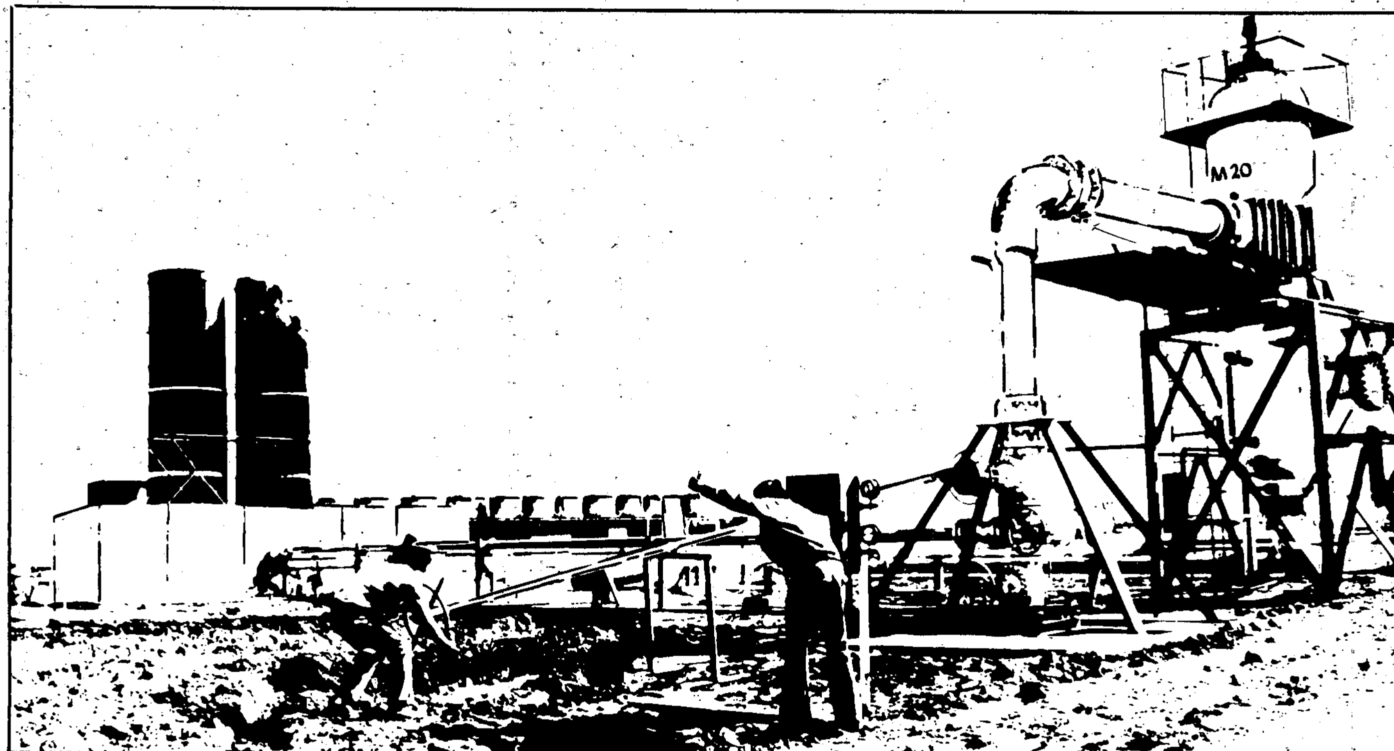

NUMERICAL MODELING STUDIES OF THE CERRO PRIETO RESERVOIR

M. J. Lippmann and K. P. Goyal

February 1980

A Joint Project of

COMISION FEDERAL DE ELECTRICIDAD
Mèxico

DEPARTMENT OF ENERGY
Division of Geothermal Energy
United States of America

Coordinated by

Coordinadora Ejecutiva
de Cerro Prieto
Apdo. Postal No. 3-636
Mexicali, Bja. Cfa., México
and P. O. Box 248
Calexico, Ca. 92231

Lawrence Berkeley Laboratory
Earth Sciences Division
University of California
Berkeley, California 94720

Operating for the U.S. Department of Energy under Contract W-7405-ENG-48

DISCLAIMER

Submitted to the Proceedings of the
Second Symposium on the Cerro Prieto
Geothermal Field, Baja California, Mexico
October 17-19, 1979

NUMERICAL MODELING STUDIES OF THE CERRO PRIETO RESERVOIR

M. J. Lippmann and K. P. Goyal

Lawrence Berkeley Laboratory
University of California
Berkeley, California 94720

NUMERICAL MODELING STUDIES OF THE CERRO PRIETO RESERVOIR

M. J. Lippmann and K. P. Goyal
Lawrence Berkeley Laboratory
University of California
Berkeley, California 94720

ABSTRACT

A prerequisite to any meaningful numerical simulation of the behavior of a geothermal system under different production management schemes is knowing the system's initial and prevailing boundary conditions.

Based on existing data, different boundary conditions and material properties were simulated using a computer program to calculate heat and mass transport in liquid-saturated nonisothermal media. In these simulations, we assumed that initially Cerro Prieto was essentially a one-phase (liquid-dominated) geothermal system.

We computed steady-state temperatures for various assumed preproduction recharge and discharge boundary conditions. The results are discussed and compared with published initial temperature distributions in the Cerro Prieto system.

INTRODUCTION

The Cerro Prieto geothermal field is presently producing 150 MW of electric power. In April 1979 the capacity of the power plant was doubled (from 75 to 150 MW) as two new units came into operation. Consequently the fluid production rate has increased from about 2800 to 4200 tonnes per hour. Bermejo M. et al. (1979) estimate that about 1.2 x 10^8 tonnes of steam-brine mixture has been extracted from the field as of late 1978. Figure 1 shows the location of over 60 deep wells that have been completed in the field.

By 1985 the Comisión Federal de Electricidad expects to increase the cumulative plant capacity at Cerro Prieto to 400 MW. Improved estimates of the total capacity of the field will be essential in studying the feasibility of further developments of the area.

A realistic geohydrological model is of fundamental importance to estimate the capacity and longevity of the Cerro Prieto field. A number of papers in this volume discuss the various efforts under way to determine the dimensions, structure and stratigraphy of the field, the properties and interconnection between the various aquifers, and the circulation of fluid and heat within the geothermal system and across its boundaries.

The purpose of this study is to establish the preproduction recharge and discharge conditions of the field. As a first step, a simplified geological model of the system was developed on the basis of the available data. Then, the heat and mass flow through this model was calculated numerically using a computer program. The location, temperature, and strength of the reservoir recharge and discharge areas, the thermal and hydraulic boundaries of the model, and the properties of the different materials were varied in an attempt to reproduce the preproduction temperatures given by Mercado G. (1976), and Elders et al. (1978). No effort was made to match early reservoir pressures since pre-1973 pressure data are only available for few wells in the central part of the field (Sánchez R. and de la Peña L., 1980).

The sources and sinks identified by this study could also be used for simulating the behavior of the field after 1973. However, their

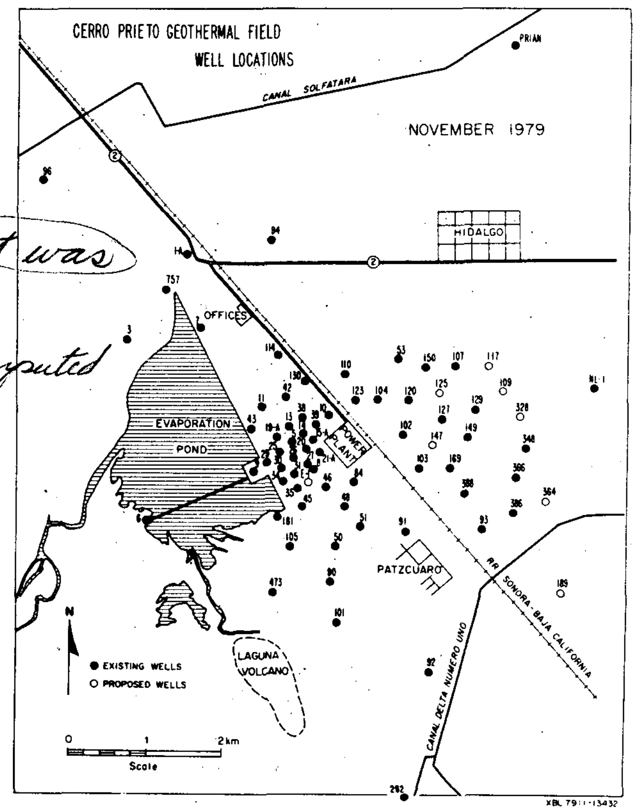

Figure 1. Well locations at the Cerro Prieto geothermal field, as of November 1979.

characteristics would change due to large-scale production. The mass inflow from the sources into the reservoir is expected to increase significantly in this open system and a decrease is anticipated at the sinks due to exploitation. In addition, areas surrounding the producing reservoir are also expected to drain (cold or hot) fluids in response to the changes in the pressure distribution in the field.

RELEVANT WORK

Knowledge about the recharge and discharge characteristics of the field is essential to predict its future behavior. Based on data from recent and earlier studies, zones of recharge and directions of flow of the recharged fluid may be inferred. Unfortunately not all the data point to exactly the same zones and directions.

On the other hand, no precise locations at depth are available for the zones where some of the fluid and heat transported across the geothermal reservoir find their way to the surface. It is safe to say that heat is conducted through the caprock, and that fluids and heat carried by convection are discharged to the surface along the main fault zones in the area.

Using well temperatures, pressures, enthalpy, flow data, and geothermochemical correlations of the fluids discharged by the wells, Mercado G. (1976) developed a hydrogeological model of the Cerro Prieto area. He postulated that: (1) hot fluids ascending in the eastern and central zones of the field flow toward the west, (2) the heat source is located in the eastern and deeper part of the field, (3) the reservoir is recharged mainly from the west (in the area of alluvial fans of the Sierra Cucapa) and also to some extent from the east by the underflow of the Colorado River water. Figures 2 and 3 show the preproduction temperature distributions in the field along two different cross-sections (Mercado G., 1976).

According to Truesdell et al. (1979b) the comparison of measured deuterium contents of the Cerro Prieto geothermal waters and the inter-

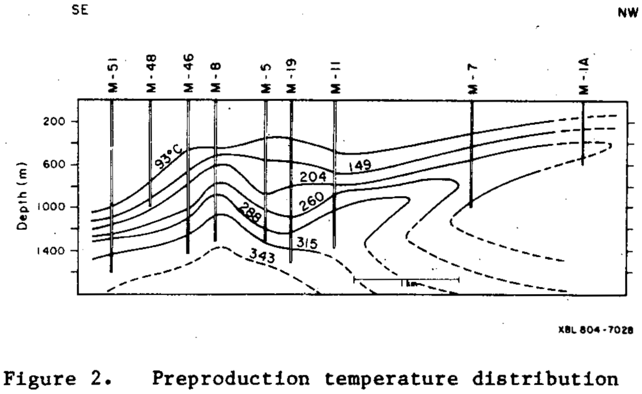

Figure 2. Preproduction temperature distribution in the reservoir along a southeast-northwest cross-section (adapted from Mercado G., 1976).

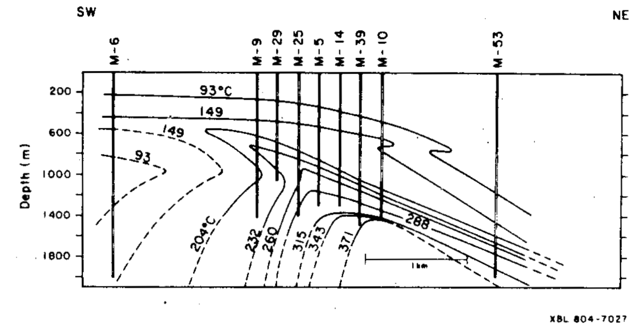

Figure 3. Preproduction temperature distribution in the reservoir along a southwest-northeast cross-section (adapted from Mercado G., 1976).

polated composition of cold Mexicali Valley ground waters suggests that the recharge to the system could have occurred along a narrow zone running from Mexicali on the north, passing just west of the field, and curving northeast to the Mesa Arenosa on the east. This recharge from the west agrees with part of Mercado's (1976) model.

Corwin et al. (1979) correlated the dipolar self-potential anomaly detected in the Cerro Prieto area with geothermal activity. They concluded that the surface anomaly could be the result of a vertical fault or fracture zone along which a vertical component of fluid and/or heat flow exists. Figure 4 shows the self-potential anomaly and the inferred location of the geological discontinuity. Based on these data the hot water upflow zone is distributed along an approximately north-south area passing near well M-48.

Elders et al. (1978) recognized a number of regularly distributed mineral zones in the field by examining cores and drill cuttings. They developed maps indicating depths to the first occurrence of some temperature diagnostic minerals. For example, Figure 5 shows the plot corresponding to epidote indicating the depth to the 230 to 250°C temperature zone. The mineral distributions suggest that the hottest fluids rose along a north-south trending zone passing near well M-105. This zone is displaced toward the west with respect to the one inferred from the self-potential study (Corwin et al., 1979).

It should be recognized that the isotopic and mineralogic data represent the preproduction condition of the system--that is, before 1973 when large-scale exploitation of the field began.

NUMERICAL COMPUTER PROGRAM AND METHODOLOGY

The numerical computer code CCC developed at Lawrence Berkeley Laboratory was used in these studies. The program solves the heat and mass flow equations for liquid-saturated media. Details on the Integrated Finite Difference Method and on explicit-implicit iterative procedure to advance in time used in this program are given given elsewhere (Edwards, 1972; Narasimhan and Witherspoon, 1976; Lippmann et al., 1977).

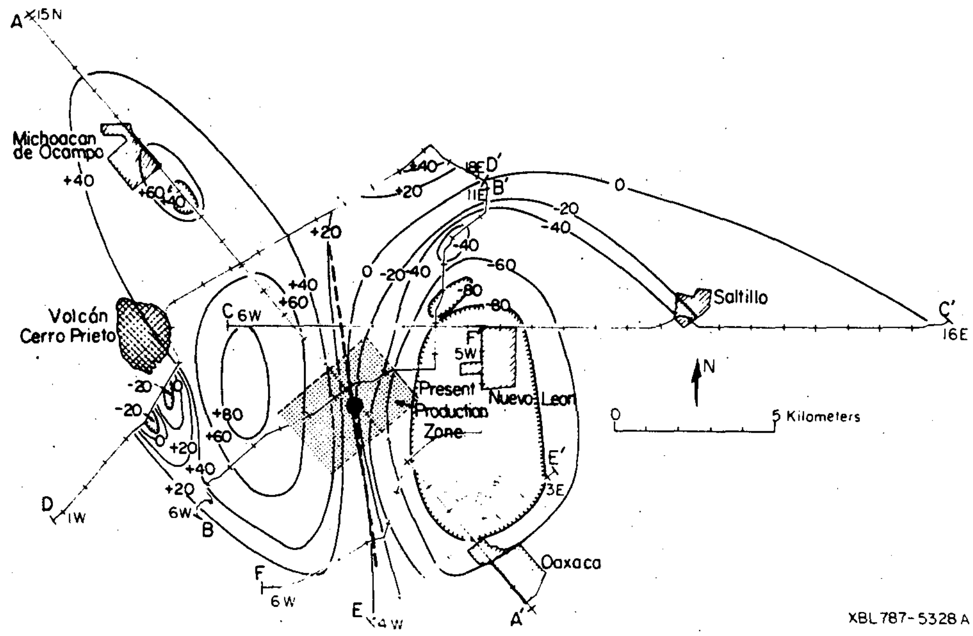

Figure 4. Self-potential contours in the Cerro Prieto area. Lines A-A′ through F-F′ are survey lines. The heavy dashed line represents the trace of the inferred self-potential source plane and location of a possible geological discontinuity. The heavy dot indicates the center of the source region (from Corwin et al., 1979).

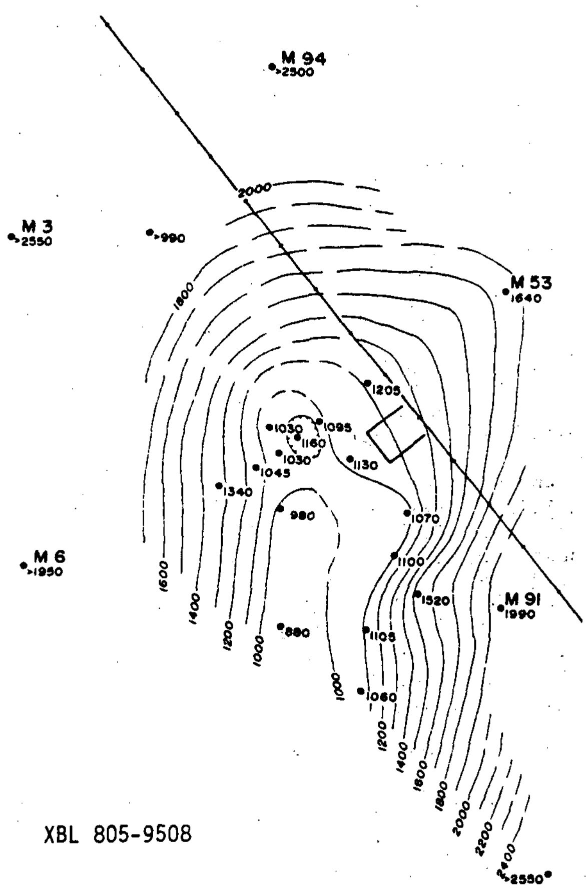

Figure 5. Depth to the first occurrence of epidote in sandstone (from Elders et al., 1978).

In all cases the numerical computations were run until a steady-state pressure and temperature distribution was obtained in the simulated system. The computed temperatures were then compared with Mercado's (1976) temperature distributions (Figs. 2 and 3).

Using these comparisons as a guide, the characteristics of the sources, sinks, and boundary conditions were modified to improve the match. The changes were not arbitrarily made but were based on available geological and reservoir engineering information.

A number of different models were used to reproduce Mercado's preproduction temperature distributions. Only the results of two of the cases studied will be discussed here. As will be shown, it was not possible to reach good agreements. We suspect that the simplified geological model and boundary conditions used in the simulations contributed to the poor matches obtained. Recent studies (Lyons and van de Kamp, 1980) indicate that the lithology of the field is quite complex, with lithofacies changes controlling largely the fluid flow within the system.

GEOLOGICAL MODEL

Using the information available in mid-1979, a simplified geological model of Cerro Prieto was developed for use in simulations. The faults believed to be bounding and intersecting the area initially developed by CFE (Cerro Prieto I) are shown on Figure 6. Based on these data, the region modeled to reproduce the preproduction conditions of the field was restricted to the area indicated on Figure 7.

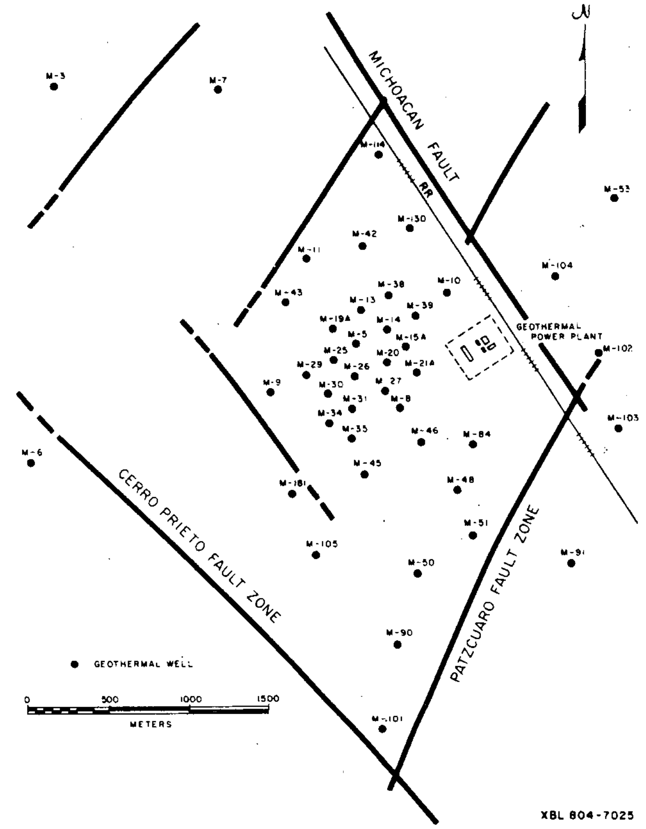

Figure 6. Fault map for the area initially developed at Cerro Prieto (from Vonder Haar and Howard, 1980).

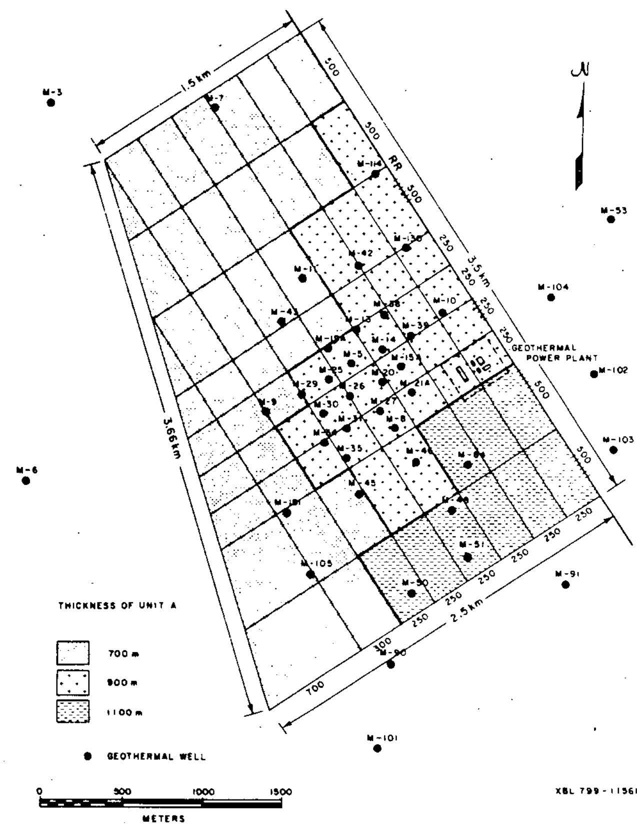

Figure 7. Plan view of the area modeled and the mesh used in this paper. Contrasting hatchings correspond to different thicknesses of Unit A (unconsolidated sediments).

Basically, the lithologic column introduced by Abril G. and Noble (1979) was incorporated in the model (Fig. 8). According to them, in this area the column may be subdivided into three units. The upper one (Unit A) consists of unconsolidated sediments, the middle one (Unit B) of consolidated materials, and the lower one (Unit C) of granodioritic and metamorphic rocks. Unit A acts as the leaky caprock of the geothermal system, while Unit C constitutes its impermeable bedrock. Unit B, overlying the basement formed by alternating sandstone and shale layers, can be divided into five major subunits.

The top layer, L_1, consists of sandstone lenses and shales. Its lenticular aquifers supposedly could be the source of colder, less saline waters which recharge the geothermal reservoirs below, as their pressures drop in response to fluid extraction (Truesdell et al., 1979a). Below Layer L_1 is Layer L_2, which is characterized by rocks with high content of carbonate cement. The underlying sandy strata, separated by a shaly layer, are the main geothermal reservoirs A and B at Cerro Prieto.

The total thickness of the sedimentary column varies within the Cerro Prieto field. Bedrock was reached only in wells M-3 (2532 m), M-96 (2713 m), and S-262 (1470 m). The depth to the block-faulted basement increases significantly toward the east (Fonseca L. and Razo M., 1980). For simulation purposes the top of the bedrock was assumed to be at a constant depth of 2500 m throughout the modeled area.

An isopach map of Unit A, based on data provided by CFE, is given in Figure 9. For the simulations the variable thickness of this unit was modeled as shown in Figure 7. By assuming constant thicknesses for the different subunits of Unit B, three basic lithologic columns were used in the model (Fig. 8). It is believed (A. Mañon M., personal commun.) that in the central part of the Cerro Prieto I area there is preferential fluid movement in a northeast-southwest direction due to presence of more permeable facies or highly fractured rocks. This feature was incorporated in the model as discussed below.

MESH USED IN THE SIMULATIONS

The three-dimensional region studied was subdivided into 560 nodes (or elements). The vertical column, 2500 m thick, was subdivided into 8 horizontal levels (each having 70 nodes). The lowest level (100 level) is 600 m thick, above it the 200 to 700 levels each 200 m thick, and the upper level (800 level) is 700 m thick. The different thick-

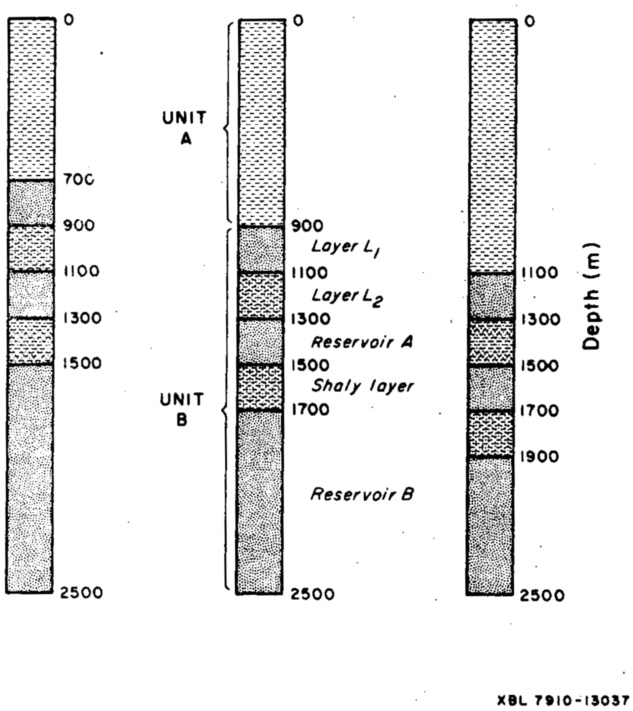

Figure 8. Basic lithologic columns used in the model for the areas with different Unit A thicknesses (see Fig. 7).

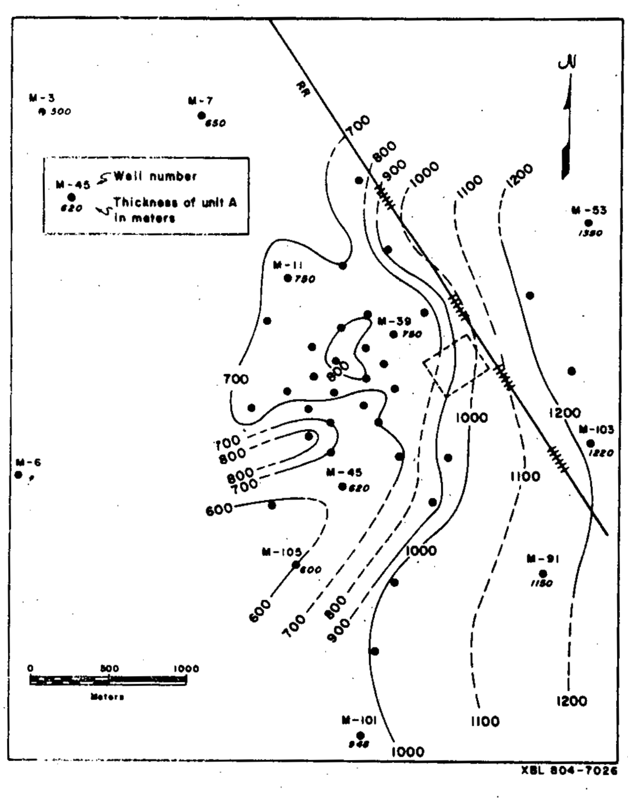

Figure 9. Unit A isopach map.

nesses were needed to account for the different lithologic columns used in the model (Fig. 8).

Figure 10 depicts the numbering used for the nodes in the 400-level, a similar numbering scheme was used in the other levels. In this three digit system, the first digit represents the level, while the number of the node is represented by the other two. Thus, node 818 lies in the 800-level layer and is vertically above nodes 118, 218, 318, 418, 518, 618, and 718. In the horizontal plane, its shape is exactly the same as that of node 418. Figure 10 shows the northeast-southwest trending high permeability area, representing a coarser facies or a fractured zone in the field. The higher permeable material was restricted to the 400 level only.

BOUNDARY AND INITIAL CONDITIONS

Boundary conditions which have to be specified in the model are: (1) type of boundaries whether open or closed to heat and mass flow, (2) temperatures and pressures at the boundaries, (3) location and strength of sources and sinks, and (4) temperature of fluid entering the system.

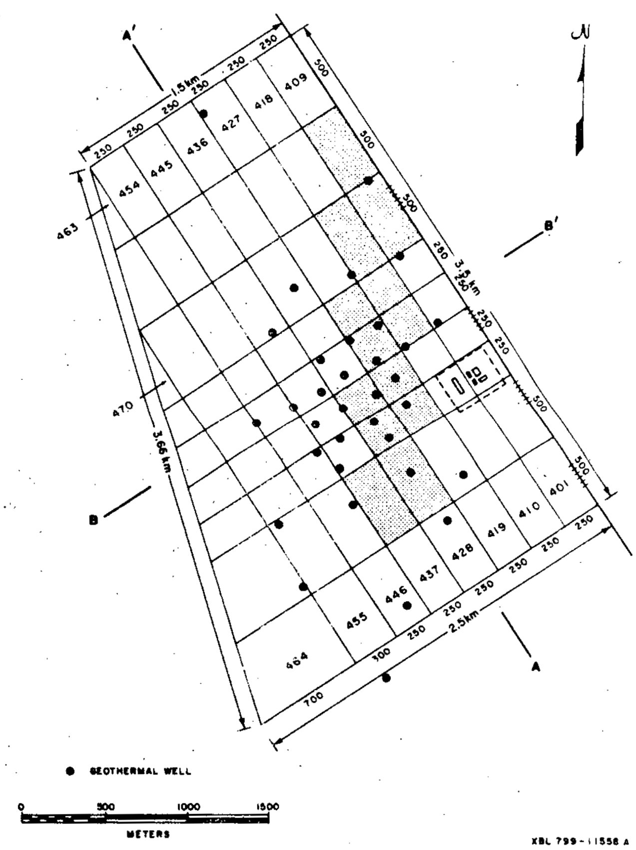

Figure 10. Plan view of the mesh used for computation. Hatched area indicates an area of higher permeability in the 400 level (1400 m depth). Node numbering for the 400 level, and the location of the A-A′ and B-B′ cross sections are also shown.

In the various models developed for the Cerro Prieto I area most of these conditions were varied to study their effect on the preproduction temperature distributions. However, in both cases discussed here, we used the following conditions: (1) The inflow and outflow of fluids into and from the region were modeled by placing sources and sinks in some nodes located at the boundaries (i.e. near geologic faults). (2) All vertical boundaries were closed to heat flow. (3) The top and bottom boundaries were held at constant temperatures. The top surface was assumed to be at 25°C; the bottom either at 150°C or 280°C. (4) The total mass flow rate across the model (from the sources towards the sinks) was arbitrarily assumed to be 2.95×10^7 kg/day. This rate is about 2.15 times the preproduction discharge of the surface manifestations in the area as reported by Mercado G. (1968). We considered that before 1973 a significant fraction of the heat and mass inflow into the geothermal field rose to the surface mainly through the fault zones.

Hydrostatic pressure and linear temperature-depth distribution were used as initial conditions for the system.

FLUID AND ROCK PROPERTIES

We assumed that (1) the fluid in the system was liquid and had constant properties, and (2) the properties of the solid matrix are isotropic and constant.

For the fluid, pure water properties at 250°C were used. The solid matrix properties are given in Table 1 and are representative of the different lithologies included in the model.

No temperature or pressure dependency of the properties was used to reduce the cost of computations, and we felt that this simplification would not significantly affect the computed steady-state temperature distributions. We planned to include temperature and pressure dependencies once an acceptable match between computed and published (Mercado G., 1976) temperatures was obtained.

Model 1

In model 1 as well as in the one discussed later, we considered that the recharge and discharge areas were closely associated with the bounding faults. We assumed the inflow of fluids into the system to be distributed as follows (Table 2):

1. 22% of the total mass recharge is at 350°C. The sources are located in the lower part of Reservoir B (100 level), near the intersection of the Michoacán and Pátzcuaro faults (Fig. 6).

2. 61% of the recharge comes from colder water sources located in the upper part of Reservoir B (levels 200 and 300, at 208°C and 188°C, respectively), near the southwest region of the system, along the Cerro Prieto fault zone.

3. 17% of inflow of fluid is concentrated at the intersection of the Michoacán fault and a northeast-southwest trending fault (Fig. 6). The 250°C source (node 608) is located in Layer L_1.

The sinks where the fluids leave the system were distributed around its northwest and southwest corners, near the intersection of the Cerro Prieto fault and northeast-southwest trending faults. The discharge occurs through Layers L_1 and L_2, at levels 700 and 500 respectively. The sinks were arranged in a manner approximately similar to the surface distribution of the geothermal manifestations in the area given by Mercado G. (1968).

The bottom of the model (2500 m depth) was considered to be a constant temperature boundary at 150°C. This low value was used to duplicate

TABLE 1. PROPERTIES USED FOR THE SOLID MATRIX

Material	Density (kg/m^3)	Heat capacity J/kg·°C	Thermal cond. (J/m·day·°C)	Intrinsic permeability (md)	Porosity
Unit A	2500	935	1.92×10^5	10^{-3}	0.20
Layer L_1	2650	825	2.8×10^5	20	0.10
Layer L_2	2700	860	1.85×10^5	5	0.10
Reservoir A	2650	825	2.8×10^5	50	0.10
Shaly layer	2700	860	1.85×10^5	5	0.10
Reservoir B	2650	825	2.8×10^5	80	0.10
Highly permeable layer	2650	825	2.8×10^5	100	0.10

TABLE 2. MODEL 1 - LOCATION AND CHARACTERISTICS OF SOURCES AND SINKS

SOURCES

Node	Mass Flow Rate (kg/day)	Temperature (°C)
101	2.5×10^6	350
110	2.5×10^6	350
119	1.5×10^6	350
264	2.5×10^6	208
265	2.5×10^6	208
266	1.5×10^6	208
267	1.5×10^6	208
268	1.0×10^6	208
364	2.5×10^6	188
365	2.5×10^6	188
366	1.5×10^6	188
367	1.5×10^6	188
368	1.0×10^6	188
608	5.0×10^6	250

SINKS

Node	Mass Flow Rate (kg/day)
527	1.00×10^6
536	1.00×10^6
545	1.00×10^6
554	1.00×10^6
562	2.00×10^6
563	0.50×10^6
564	3.50×10^6
565	2.75×10^6
566	2.00×10^6
727	1.00×10^6
736	1.00×10^6
745	1.00×10^6
754	1.00×10^6
762	2.00×10^6
763	0.50×10^6
764	3.50×10^6
765	2.75×10^6
766	2.00×10^6

the temperatures of the regions away from the hot recharge zones. Around the inflow zones the temperatures near the bottom of the model will be reflecting those of the recharge fluids and not that of the boundary.

The computed steady-state temperatures are described by various temperature distribution maps. The effect of sources and lower permeability layers on the fluid flow can be established by analyzing the isotherms at different depths. The hotter waters entering the system at the deeper levels move in response to the pressure distribution resulting from the sources and sinks located in the model; it tends to move around the less permeable layers.

The isotherms at 1000 m (600 level) and 1400 m (400 level) are given in Figures 11 and 12, respectively. In Figure 11 the 250°C isotherm in the northeast part reflects the effect of the source in node 608. The high temperatures in the south-central part of the system are caused by the hot water rising from beneath. In Figure 12, the

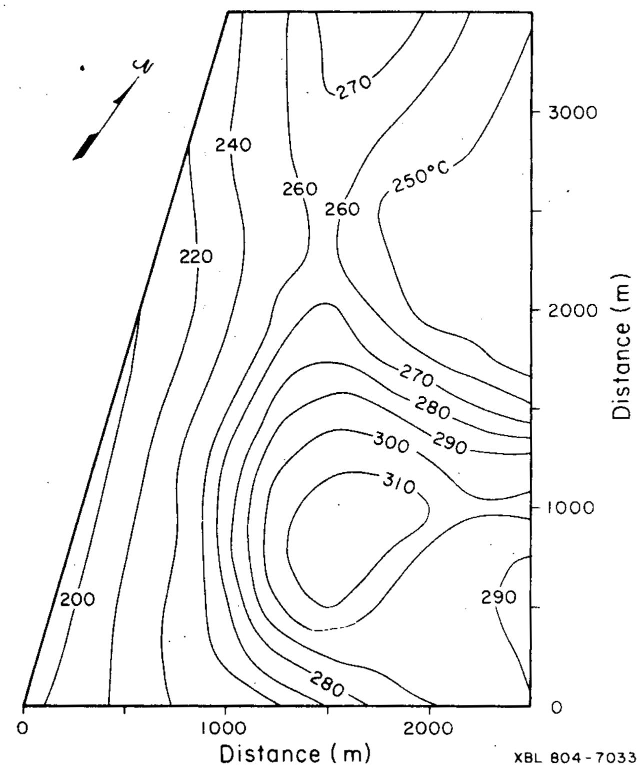

Figure 11. Model 1. Isothermal map for the 600 level (1000 m depth).

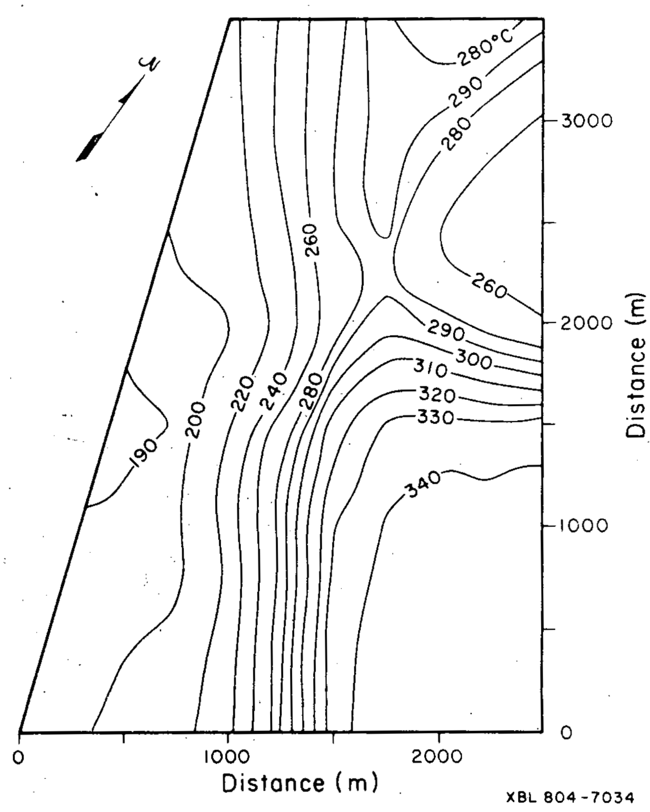

Figure 12. Model 1. Isothermal map for the 400 level (1400 m depth).

isotherms in the southeast corner indicate the movement and cooling of the water as it flows away from the 350°C sources. The 190°C isotherm toward the west shows the influence of 188°C sources located in the 300 level; the 260°C isotherm toward the northeast shows that of 250°C sources in the 600 level.

The calculated temperatures along the sections A-A′ and B-B′ (Fig. 10) are shown in Figures 13 and 14. These plots, when compared with the temperatures given in Figures 2 and 3, indicate that in the southeast-northwest section, the computed temperatures are higher everywhere except in the area near the center of Figure 13. In this region the temperatures seem to be dominated by the strength and temperatures of the sources located at the southeast corner of the field. A comparison of Figures 3 and 14 indicates that the temperatures match favorably near well M-9 and in the central part of the field. Generally the calculated temperatures are higher than those of Mercado.

To determine the effect of increasing the temperature of the lower boundary of the model, it was changed from 150 to 280°C. Comparing Figures 13 and 15 shows an increase of the temperature throughout the system. The major observed temperature differences are in the lower 1500 m, in the northwest part of the section. The effects are less toward the southeast because of the presence of the fluid sources whose temperatures were kept unchanged.

By modifying the temperature of the lower boundary no improvement of the match with Figure 2 and 3 was achieved. It was decided to modify the characteristics of the fluid sources of the model to attain a closer correspondence with Mercado's preproduction temperatures.

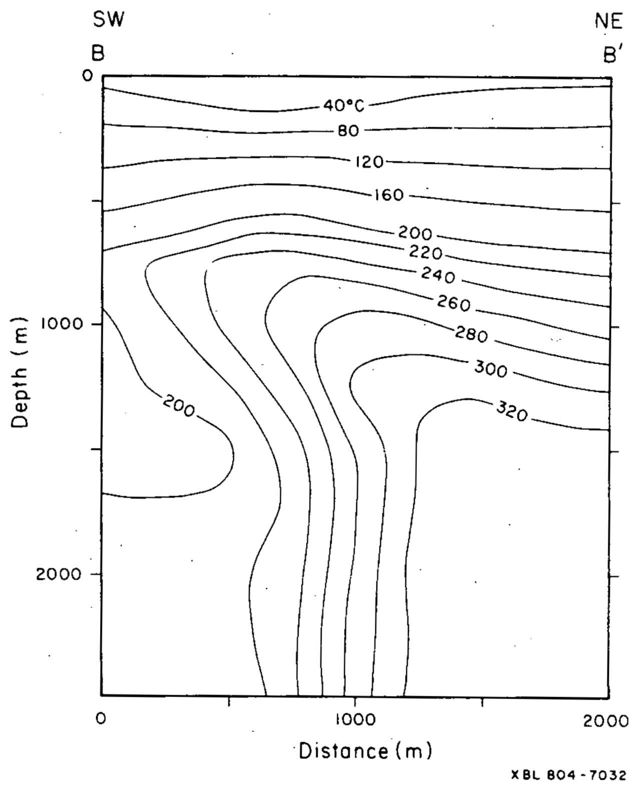

Figure 14. Model 1. Temperature distribution along the B-B′ cross section.

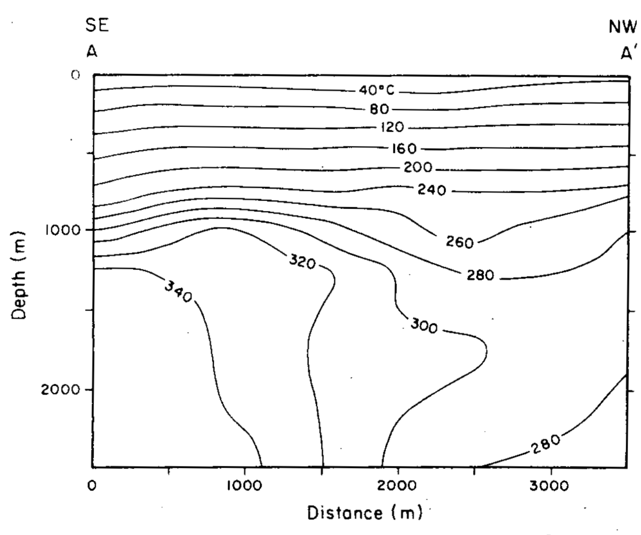

Figure 13. Model 1. Temperature distribution along the A-A′ cross section.

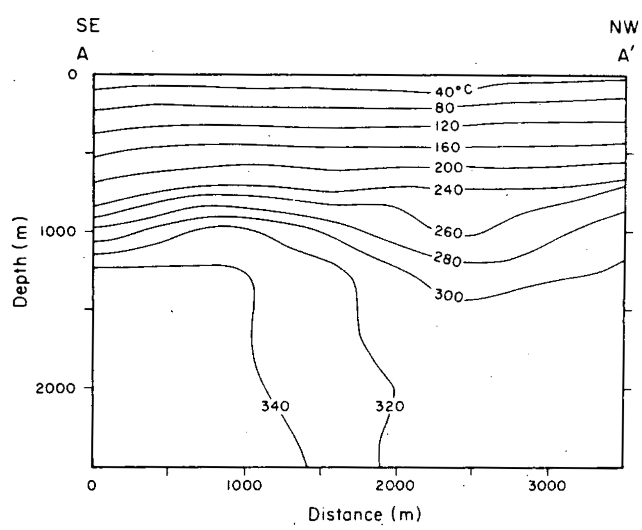

Figure 15. Model 1, with lower constant temperature boundary at 280°C. Temperature distribution along the A-A′ cross section.

Model 2

To obtain a better match, the sources in the 100 level were displaced towards the southwest corner of the system and the 200-level sources were taken out and their flow rates were added to those at the 100 level. The temperature of the sources at the 300 and 600 levels were changed to 200°C (Table 3). The sinks in this model were assumed to be equal to those in Model 1 (Table 2). The temperature of the lower boundary was again fixed at 150°C.

Isotherms at 1000- and 1400-m depths (600 and 400 levels) are given in Figures 16 and 17. Temperatures have changed with respect to those of Figures 11 and 12 in response to the change of source characteristics.

Isotherms along section A-A′ are shown in Figure 18. A comparison with Figure 2 indicates that the calculated temperatures at well M-8 are close to Mercado's. Temperatures in the central part of Figure 18 also match favorably those in Figure 2. The calculated temperatures are slightly higher in the southeastern part of the field. Isotherms along section B-B′ are shown in Figure 19. A comparison of these temperatures with those in Figure 3 shows that the calculated temperatures are, in general, higher than the preproduction temperatures given by Mercado G. (1976).

FINAL REMARKS

A simplified three-dimensional hydrogeological model of the Cerro Prieto field was developed using the available data at the time. We considered numerous modifications in the model's boundary conditions, especially in the characteristics and locations of sources and sinks, and properties of the different lithologies in the model with the purpose of matching the computed steady-state temperatures with those preproduction temperatures reported by Mercado G. (1976). Only partial matches were obtained, as illustrated in the two examples discussed above. To determine the preproduction recharge and flow characteristics of

TABLE 3. MODEL 2 - LOCATION AND CHARACTERISTICS OF SOURCES

Node	Mass Flow Rate (kg/day)	Temperature (°C)
128	2.5×10^6	350
137	3.0×10^6	350
146	3.0×10^6	350
155	3.0×10^6	350
164	2.5×10^6	350
165	1.5×10^6	350
364	2.5×10^6	200
365	2.5×10^6	200
366	1.5×10^6	200
367	1.5×10^6	200
368	1.0×10^6	200
608	5.0×10^6	200

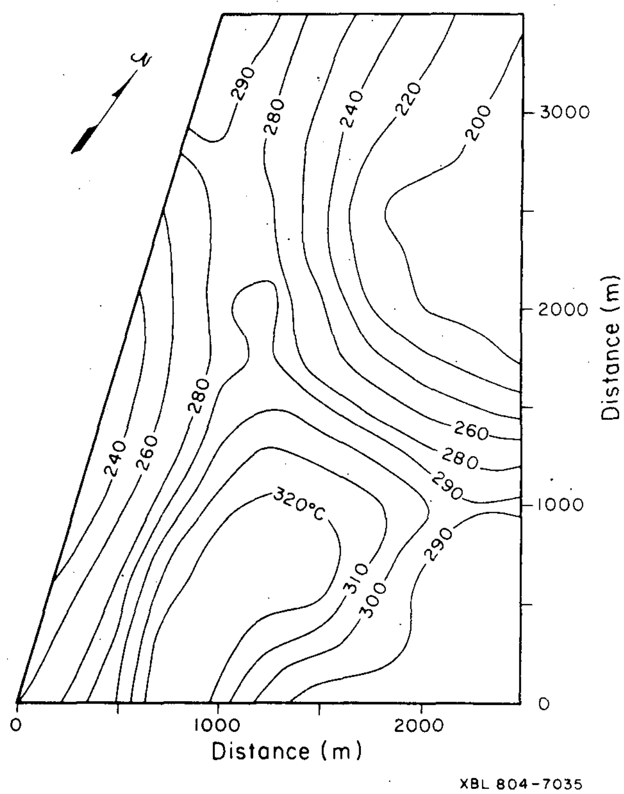

Figure 16. Model 2. Isothermal map for the 600 level (1000 m depth).

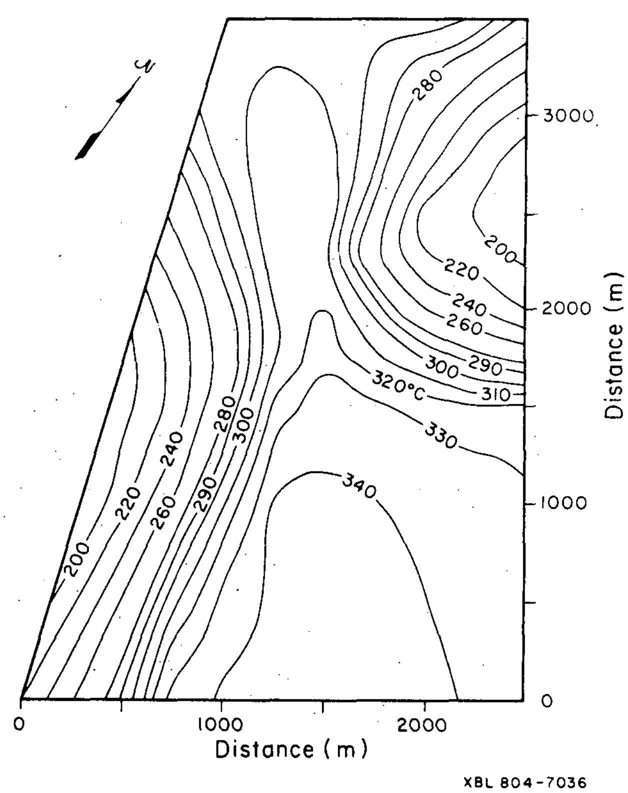

Figure 17. Model 2. Isothermal map for the 400 level (1400 m depth).

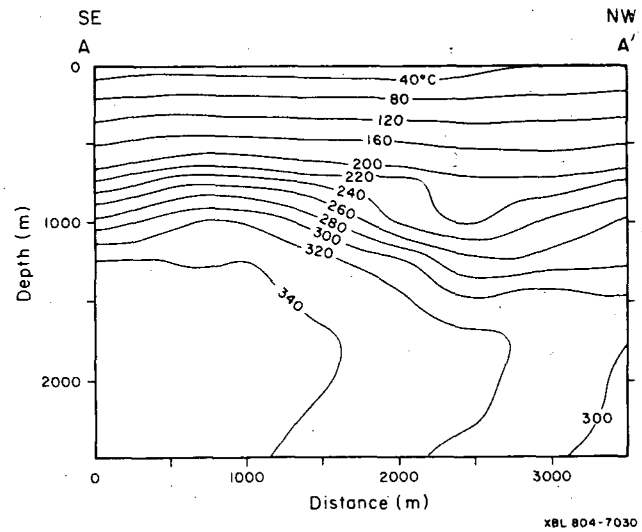

Figure 18. Model 2. Temperature distribution along the A-A′ cross section.

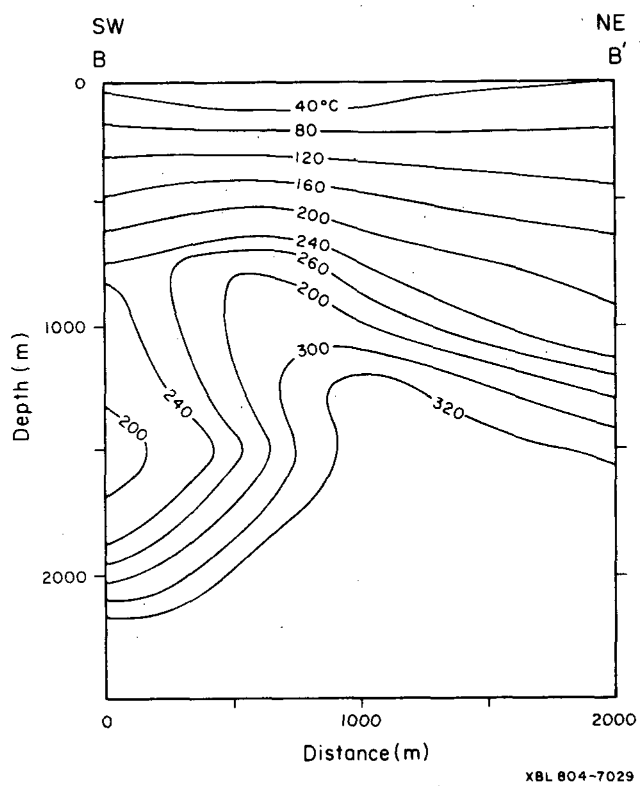

Figure 19. Model 2. Temperature distribution along the B-B′ cross section.

the field, it will be necessary to obtain not only more temperature data but also early pressure distribution data and to improve the geological model of this system.

Several authors in this volume have presented new information on the structure, lithology, and the physical characteristics of the field. The wealth of information becoming available will allow the development of an improved model of the field which could be incorporated in future simulations to establish the pre-1973 characteristics of the area and to predict the future behavior of the geothermal field as its development continues.

ACKNOWLEDGMENTS

We would like to thank our colleagues of the Coordinadora Ejecutiva de Cerro Prieto of CFE and of the Earth Sciences Division of LBL for sharing their data and for their valuable suggestions.

This work was supported by the U. S. Department of Energy, Division of Geothermal Energy, under contract W-7405-ENG-48.

REFERENCES CITED

Abril G., A. and Noble, J. E., 1979, Geophysical well-log correlations along various cross-sections of the Cerro Prieto geothermal field, in Proceedings, First Symposium on the Cerro Prieto geothermal field, Baja California, Mexico, September 1978: Berkeley, Lawrence Berkeley Laboratory, LBL-7098, p. 41-48.

Bermejo M., F., Cortéz A., C., and Aragón A., A., 1979, Physical and thermodynamic changes observed in the Cerro Prieto geothermal reservoir, in Proceedings, First Symposium on the Cerro Prieto geothermal field, Baja California, Mexico, September 1978: Berkeley, Lawrence Berkeley Laboratory, LBL-7098, p. 300-332.

Corwin, R. F., Morrison, H. F., Díaz C., S., and Rodríguez B., J., 1979, Self-potential studies at the Cerro Prieto geothermal field, in Proceedings, First Symposium on the Cerro Prieto geothermal field, Baja California, Mexico, September 1978: Berkeley, Lawrence Berkeley Laboratory, LBL-7098, p. 204-210.

Edwards, A. L., 1972, TRUMP: A computer program for transient and steady state temperature distribution in multidimensional systems: Livermore, Lawrence Livermore Laboratory, UCRL-14754, Rev. 3.

Elders, W. A., Hoagland, J. R., Olson, E. R., McDowell, S. D. and Collier, P., 1978, A comprehensive study of samples from geothermal reservoirs: Petrology and light stable isotope geochemistry of twenty-three wells in the Cerro Prieto geothermal field, Baja California, Mexico: Riverside, University of California, UCR/IGPP-78/26.

Fonseca L., H., and Razo M., A., 1980, Gravimetric magnetometric and seismic reflection studies at the Cerro Prieto geothermal field (this volume).

Lippmann, M. J., Tsang, C. F., and Witherspoon, P. A., 1977, Analysis of the response of geothermal reservoirs under injection and production procedures: Dallas, Society of Petroleum Engineers, SPE-6537.

Lyons, D. J., and van de Kamp, P. C., 1980, Subsurface geological and geophysical study of the Cerro Prieto geothermal field: Berkeley, Lawrence Berkeley Laboratory, LBL-10540 (in preparation).

Mercado G., S., 1968, Localización de zonas de máxima actividad hidrotermal por medio de proporciones químicas, campo geotérmico de Cerro Prieto B. C.: presented at the III Congreso Mexicano de Química Pura y Aplicada March 21-23, 1968, Guadalajara, Mexico: Sociedad Química de México.

Mercado G., S., 1976, Movement of geothermal fluids and temperature distribution in the Cerro Prieto geothermal field, Baja California, Mexico, in Proceedings Second United Nations Symposium on the Development and Use of Geothermal Resources, May 1975: Washington, D. C., U. S. Government Printing Office, v. 1, p. 487-494.

Narasimhan, T. N., and Witherspoon, P. A., 1976, An integrated finite difference method for analyzing fluid flow in porous media: Water Resources Research, v. 12, no. 1, pp. 57-64.

Sáncnez R., J., and de la Peña L., A., 1980, Preliminary geohydrological study of the Cerro Prieto geothermal field (this volume).

Truesdell, A. H., Mañon M., A., Jiménez S., M. E., Sánchez A., A., and Fausto L., J. J., 1979a, Geochemical evidence of drawdown in the Cerro Prieto geothermal field, in Proceedings, First Symposium on the Cerro Prieto geothermal field, Baja California, Mexico, September 1978: Berkeley, Lawrence Berkeley Laboratory, LBL-7098, p. 130-135.

Truesdell, A. H., Rye, R. O., Pearson, F. J. Jr., Olson, E. R., Nehring, N. L., Huebner, M. A., and Coplen, T. B., 1979b, Preliminary isotropic studies of fluids from the Cerro Prieto geothermal field, in Proceedings, First Symposium on the Cerro Prieto geothermal field, Baja California, Mexico, September 1978: Berkeley, Lawrence Berkeley Laboratory, LBL-7098, p. 95-99.

Vonder Haar, S., and Howard, J. H., 1980, Intersecting faults and sandstone stratigraphy at the Cerro Prieto geothermal field (this volume).

TECHNICAL INFORMATION DEPARTMENT
LAWRENCE BERKELEY LABORATORY
UNIVERSITY OF CALIFORNIA
BERKELEY, CALIFORNIA 94720